First-Principles Calculation of Lattice Stability of C15-M_2R and Their Hypothetical C15 Variants (M=Al,Co,Ni; R=Ca,Ce,Nd,Y)

Michael C. Gao[1*], Anthony D. Rollett[1], Michael Widom[2]

[1]Department of Materials Science and Engineering, [2]Department of Physics, Carnegie Mellon University

5000 Forbes Ave, Pittsburgh, PA 15213, USA

* Corresponding author. Email: mgao@cmu.edu. Tel: +1-412-268-2692; Fax: +1-412- 268-7596.

Abstract

When combining a stoichiometric Laves phase C15-A_2B_1 with a solid solution C15 phase(s) into a multi-component system, a sublattice remodeling of the $(A,B)_2(A,B)_1$ compound is needed for the sake of database compatibility. This then requires a set of physically-grounded thermodynamic parameters for the hypothetical C15-variants (in the simplest case, A_2A, B_2B, and B_2A), in order to avoid distortion of the phase field relating to the C15 phase in the A-B phase diagram due to the sublattice remodeling. For this purpose, the present investigation employed first-principles (FP) calculations to study the lattice stability of the stable binary C15-M_2R (M=Al, Co, Ni; R=Ca, Ce, Nd, Y) and their hypothetical (unstable) C15 variants at T=0 K. Our results demonstrated that use of the empirical parameters and energy constraint commonly used in the literature leads to a too large homogeneity range in some of the systems studied and, consequently, significant distortions of the phase diagram. In contrast, when enthalpies of formation based on FP calculations were used for the hypothetical C15 phases, such distortion of

the phase diagram is minimized. The other advantage is that there is no need for re-optimization of the existing thermodynamic databases. Therefore, it is proposed that FP enthalpies of formation should be used for the thermodynamic descriptions of hypothetical C15 phases, at least when the empirical parameters fail to reproduce a reasonably accurate A-B binary phase diagram.

Keywords: First-Principles; CALPHAD; Enthalpy of Formation; C15 Laves Phase; Hypothetical Lattices

1. Introduction

The handbook of binary alloy phase diagrams [1,2] treats many Laves C15-A_2B compounds (Pearson symbol cF24, prototype Cu_2Mg) as stoichiometric because their homogeneity range, if present, is negligible. This includes all the C15-Al_2RE, TM_2RE, Al_2Sc and Al_2Y compounds, where TM signifies a transition metal and RE signifies a rare earth element. Therefore, these C15 compounds can be modeled with a 2-sublattice model of type $(A)_2(B)_1$ for thermodynamic assessment (each pair of parentheses represents one sublattice; the subscript represents the nominal chemical formula), since a C15 lattice consists of only two crystallographic sites (A atoms occupy Wyckoff sites 16d and B atoms occupy 8a). However, other C15 phases (typically TM_2TM, e.g. Fe_2Zr [3] or TaV_2 [4]) do show an appreciable homogeneity range, which can be modeled with a sublattice of type $(A,B)_2(A,B)_1$. Component A mainly occupies the 1st sublattice, and component B mainly occupies the 2nd sublattice, but both A and B are allowed to substitute for each other in each sublattice.

When combining an A-B system that has a stoichiometric C15-A_2B compound with another system(s) that has a solid-solution C15-C_2A (e.g.) compound to form a multi-component system, a sublattice model of either $(A,C)_2(A,B,C)_1$ or $(A,B,C)_2(A,B,C)_1$ can be chosen for the C15 phase for database compatibility. Then, a set of thermodynamic parameters for the hypothetical C15 lattices (in the simplest case, C15-A_2A, -B_2A, and -B_2B) are required. The common practice in the CALPHAD community is to set the enthalpy of formation equal to a constant positive value of +5000 J/mol for the hypothetical C15 end members, and the Gibbs energy of the antiphase is determined by an energy constraint, which states that the sum of Gibbs energy of C15-A_2B and B_2A lattices should equal that of the C15-A_2A and B_2B lattices [3-7, see Eq. 7 in this report][1]. A review of the crystal structures of, and thermodynamic descriptions appropriate to topologically close packed (TCP) phases, including Laves phases C14, C15 and C16, can be found in Ref. [5].

However, the arbitrarily chosen value of +5000 J/mol for the hypothetical C15 end members [3-7] is very different from those that are determined from FP calculations (e.g., in Al-Ca [8]). Moreover, the phase diagrams constructed with this value of formation enthalpy sometimes show an exaggerated range of C15 phase stability (e.g., in Al-Ce, Al-La and Al-Nd systems [6,7]). The reason is that this empirical choice of formation enthalpy overestimates the stability of the hypothetical C15 lattices. Since this quantity is not accessible in experiments, FP calculations provide an essential alternate source of thermodynamic data for multicomponent computational thermodynamics. It was therefore a natural extension of a current investigation of the energetics of stable C15-M_2R (M=Al, Co, Ni; R=Ca, Ce, Nd, Y) compounds using FP [9], to

obtain the energetics of the corresponding phases with the hypothetical lattices. The calculated energies for the hypothetical lattices from FP together with appropriate empirical parameters were then substituted into the corresponding M-R thermodynamic database to check their impact on the associated M-R binary phase diagram. Certain M-R systems, including Al-Ca [10], Al-Ce [9], Al-Nd [9], Al-Y [11], Ce-Co [12], Nd-Ni [13] and Ni-Y [14] systems were selected for thermodynamic re-assessment. The equilibrium phase diagrams were calculated using the Thermo-Calc® software [15].

2. First-principles energy calculations

The lattice stability of the C15 phases and their hypothetical unstable variants (end members and antiphases) were analyzed using the FP code-Vienna Ab-initio Simulation Package (VASP) [16,17], which solves for the electronic band structure using electronic density functional theory (DFT) [18] on a plane-wave basis. DFT replaces the many-electron wave function with a set of single-electron wave functions, each interacting with the effective charge density of the others. Although DFT can be exact in principle, in practice this effective interaction is unknown and must be approximated using exchange-correlation potentials that describe the effects of the Pauli principle and the Coulomb potential. Popular choices of exchange-correlation potential and its dependence on electron density are based on either the local density approximation (LDA) or a generalized gradient approximation (GGA). The results of DFT calculations include the total energy of a structure, and the forces acting on each atom.

[1] All Gibbs energies are expressed in the unit of J/mol of total atoms in this report unless otherwise specified.

Many details of our approach are outlined in Ref. [19]. Because of the presence of RE elements Ce and Nd, we use the projector augmented wave (PAW) potentials [20]. These are similar to pseudopotentials except that the core electrons are solved simultaneously with the valence electrons. We use the Perdew-Burke-Ernzerhof (PBE) gradient approximation [21] to the exchange-correlation functional. Two choices are available for each RE potential, a "standard" version in which the entire set of f-levels is treated within the valence band, and a trivalent version (named "Ce_3" and "Nd_3") in which some f-electrons are kept frozen in the core. Since the Ce_3 potential predicts a positive enthalpy of formation (ΔH_f =+5.7 kJ/mol) for the stable C15-$CeCo_2$ compound, the standard Ce potential was used throughout the Al-Ce-Co system. However, we also noticed that Ce_3 potential works well for certain other systems that we studied involving Ce. On the other hand, the enthalpies of formation for hypothetical C15 Nd_2Nd (ΔH_f =+7.3 kJ/mol) and Nd_2Al (ΔH_f =+2.3 kJ/mol) resulting from the standard Nd potential are very small compared with those of C15-Ce_2Ce/Y_2Y and $AlCe_2$/AlY_2, respectively (see Table 1). Therefore, the Nd_3 potential was used throughout the Al-Nd-Ni system, which yielded a consistent set of data of enthalpies of formation for the stable and hypothetical C15 lattices. The rationale for the choice of RE potential is based on the fact that the values of ΔH_f for stable C15-Al_2RE that were experimentally measured are all comparable [22]. This is not surprising since all the RE, especially the early rare earth elements, are chemically close to each other, therefore, it can be physically argued that the values of ΔH_f for the hypothetical C15-RE_2Al and C15-RE_2RE lattices should be comparable to each other. We think the standard Nd potential is responsible for the abnormally small values for the hypothetical C15-Nd_2Nd and Nd_2Al lattices, although the calculated enthalpies of formation for stable Al-Nd binary compounds are all reasonable with standard Nd potential.

Reciprocal space (k-point) meshes were refined to achieve convergence to a precision of 1 meV/atom, and the lattice parameters were optimized. Because of the high symmetry of the C15 structures that were studied (namely C15-M_2M, R_2M and R_2R, rather than $(M,R)_2R_1$ or $M_2(M,R)_1$ or $(M,R)_2(M,R)_1$ with partial occupancy of each component in at least one sublattice), atomic coordinates (fractional units) do not relax. The plane-wave energy cutoff was held constant at the default potentials: 240 eV for Al-Ca; 268 eV for Al-Ce-Co; 270 eV for Al-Nd-Ni and Al-Ni-Y systems. The uncertainty in the value of enthalpy of formation in this report is less than 10 meV/atom (about ±1 kJ/mole of total atoms). All the calculations were performed with "medium" precision without lowering the overall accuracy; more details on choice of precision is described in the Appendix. Spin polarization was considered in all calculations involving the elements Ce, Co, Nd or Ni, but its effect on the magnetic spin momentum and enthalpy of formation is not seen in any compound studied with standard Ce and Nd_3 potentials. (When the standard Nd potential is used, the resulting magnetic spin moment is 1.211 Bohr magnetons per atom for Al_2Nd and 1.095 for Ni_2Nd compounds.)

To obtain enthalpy of formation values, ΔH_f, a composition-weighted average of the pure elemental cohesive energies was subtracted from the cohesive energy of a given compound. The resulting energy is an "enthalpy" because its volume is relaxed (at zero pressure). Descriptions of the methods of calculation of enthalpy of formation and structure for a binary system can be found on the WWW [23] and in Ref. [9]. The resulting enthalpies of formation for stable C15-M_2R and their hypothetical variants C15-M_2M, R_2R and R_2M are listed in Table 1. As expected, all the hypothetical lattices have a very large positive value of ΔH_f, indicating that they are truly

unstable phases when a C15 structure is imposed for their particular composition. All the calculated ΔH_f values of stable C15-M_2R compounds agree reasonably well with those determined from CALPHAD assessment (see Table 1) except for Al_2Y. It is possible that the assessment [11] may have overestimated ΔH_f of Al_2Y, since Timofeev *et al*. reported a value of -53.5 kJ/mol [24], which is fairly close to the value found in current FP calculations. The good agreement for the ΔH_f of stable C15-M_2R compounds between FP calculations and CALPHAD assessment demonstrated that it would be appropriate to incorporate FP into both CALPHAD assessment [8,25-29] and experimental phase diagram determination [9].

3. Thermodynamic models

The details of the CALPHAD models for computing a binary phase diagram can be found, for example, in Ref. [9] for Al-Ce and Al-Nd systems. The focus of this report is on C15 phase energetics with a sublattice model of $(A,B)_2(A,B)_1$, which is described as:

$$G^{C15} = {}^{ref}G^{C15} + {}^{id}G^{C15} + {}^{ex}G^{C15} \quad (1)$$

$${}^{ref}G^{C15} = y_A^I y_A^{II}\, {}^oG_{A:A}^{C15} + y_A^I y_B^{II}\, {}^oG_{A:B}^{C15} + y_B^I y_A^{II}\, {}^oG_{B:A}^{C15} + y_B^I y_B^{II}\, {}^oG_{B:B}^{C15} \quad (2)$$

$${}^{id}G^{C15} = \tfrac{2}{3}RT(y_A^I \ln y_A^I + y_B^I \ln y_B^I) + \tfrac{1}{3}RT(y_A^{II} \ln y_A^{II} + y_B^{II} \ln y_B^{II}) \quad (3)$$

where y^I and y^{II} are the site fractions of component *i* (*i=A,B*) in the first *(I)* and second *(II)* sublattices, respectively. ${}^oG_{A:B}^{C15}$ is the Gibbs energy for the stable C15-A_2B compound. ${}^oG_{A:A}^{C15}$, ${}^oG_{B:B}^{C15}$ and ${}^oG_{B:A}^{C15}$ are the Gibbs energies of the hypothetical C15-A_2A, B_2B and B_2A, respectively, and they are modeled as:

$$^{o}G_{A:A}^{A_2A} = {}^{o}G_{A}^{SER} + a_1 + b_1T \quad (4)$$

$$^{o}G_{B:B}^{B_2B} = {}^{o}G_{B}^{SER} + a_2 + b_2T \quad (5)$$

$$^{o}G_{B:A}^{B_2A} = 2/3\,{}^{o}G_{B}^{SER} + 1/3\,{}^{o}G_{A}^{SER} + a_3 + b_3T \quad (6)$$

where a_i, b_i are parameters to be determined, and $^{o}G_{A}^{SER}$ and $^{o}G_{B}^{SER}$ are the Gibbs energies of the pure components, A and B, in the Stable Element Reference (SER) state, *i.e.*, the enthalpies of the pure elements in their defined reference phase at T=298.15 K and P=1.013x10^5 Pa. In the present investigation, the excess mixing term ($^{ex}G^{C15}$), which accounts for the interaction of components A and B in each sublattice, is set to zero for simplicity. Its CALPHAD description can be found in Ref. [3-7], whose parameters can be derived from FP calculations employing techniques such as coherent potential approximation [30], cluster expansion [31-34], and special quasirandom structure calculation [35-38]. The ideal mixing term ($^{id}G^{C15}$) is related to the configurational entropy of mixing.

For intermetallic phases that exhibit small concentration of defects of anti-structure atoms or vacancies on both sublattices, Wagner [39] expressed the molar Gibbs energy of formation as a linear function of the number of defects in the different sites. Subsequently Ansara *et al.* [40] have shown that Wagner's expression is mathematically equivalent to Eq. 7:

$$^{o}G_{B:A}^{C15} = -{}^{o}G_{A:B}^{C15} + {}^{o}G_{A:A}^{C15} + {}^{o}G_{B:B}^{C15} \quad (7)$$

An important feature of Eq. 7 is that the Gibbs energy of formation of a phase with a hypothetical lattice via the substitution mechanism is correlated with the energy of its stable stoichiometric lattice. Therefore, Eq. 7 can be understood as an energy constraint among the hypothetical lattices. Since the energy constraint reduces the number of parameters to be optimized, it thus has

become a common practice for C15 phase description [3-7]. However, in general, how to determine ${}^{o}G_{A:A}^{C15}$ and ${}^{o}G_{B:B}^{C15}$ is still an open question since they are not available through experiments (by contrast, ${}^{o}G_{A:B}^{C15}$ can be determined from experiments). To overcome this difficulty, an empirical value of +5000 J/mol was assigned as ΔH_f (i.e., the parameter a_i in Eq. 4-5) to the C15 end-members with respect to the SER state (see Ref. [5] for a list of the Gibbs energy of the C15 end-members used in the literature). In summary, the empirical formation enthalpies for the hypothetical C15 lattices that are commonly used in the CALPHAD community are:

$${}^{o}G_{A:A}^{C15} = 5000 + {}^{o}G_{A}^{SER} \quad (8)$$

$${}^{o}G_{B:B}^{C15} = 5000 + {}^{o}G_{B}^{SER} \quad (9)$$

$${}^{o}G_{B:A}^{C15} = 10000 - {}^{o}G_{A:B}^{C15} + \tfrac{1}{3}{}^{o}G_{A}^{SER} + \tfrac{2}{3}{}^{o}G_{B}^{SER} \quad (10)$$

4. Results and discussion

The ternary systems Al-Ca-Cu, Al-Ce-Co, Al-Nd-Ni and Al-Ni-Y all include 2 edge C15 binary compounds (namely, C15-Al_2R and C15-TM_2R) except for Al-Ca-Cu. The C15-Al_2Ca compound is stable in the Al-Ca system, but C15-Cu_2Ca is unstable with ΔH_f = -11.0 kJ/mol at T = 0 K, a value that lies above the convex hull by +5.8 kJ/mol (= 60 meV/atom). All seven binary M-R systems have been thermodynamically assessed in the literature [6,7,9-14]. The corresponding M-R phase diagrams are represented with the solid lines in Figs. 1-7 when the M_2R phase is treated as a stoichiometric compound. The assessed thermodynamic descriptions

[9-14] were used directly and left unchanged except that the C15 phase was remodeled with a sublattice model of $(M,R)_2(M,R)_1$ to replace the stoichiometric C15-M_2R_1 description solely for the purpose of database compatibility. The Gibbs energy of the hypothetical C15-M_2M, R_2R and R_2M lattices were taken from the empirical parameters (Eq. 8-10) and FP energetics respectively for the purposes of comparison.

The resulting Al-R (R=Ca, Ce, Nd, Y) phase diagrams from the two treatments mentioned above are shown in Figs. 1-4, respectively. The use of empirical values for formation enthalpy and energy constraint result in a significant homogeneity range of Al_2Ca, Al_2Ce, and Al_2Nd, and the phase equilibria in their vicinity are greatly distorted, except for the case of the Al-Y system where the effect is small. The key point is that the remodeled C15-$(Al,R)_2(Al,R)_1$ becomes much more stable than the stoichiometric C15-Al_2R_1. Consequently, any phase field pertaining to the C15 phase (e.g. liquid+C15) becomes broader, and all the relevant invariant reactions (temperature and composition) are distorted to a significant extent. For example, the remodeled C15-$(Al,Ca)_2(Al,Ca)_1$ exhibits a wide compositional range of 30.7-43.7 at% Ca, and the temperature of the invariant peritectic reaction $Liquid + Al_2Ca \Leftrightarrow Al_{14}Ca_{13}$ is lowered by 77 ^oC when the empirical parameters and energy constraint were used. For the Al-Ce and Al-Nd systems, the homogeneity range of Al_2Ce and Al_2Nd also becomes significant at temperatures above 600 ^oC. An effort was made to optimize the thermodynamic parameters of the systems of Al-Ce and Al-Nd aiming for a better agreement with experiments (i.e., enthalpy of formation of compounds, measured invariant reactions and liquidus temperatures, etc.), but it was found to be impossible to satisfy the experimental constraints while leaving the empirical parameters unchanged. The Al-Ce (Fig. 2) and Al-Nd (Fig. 3) phase diagrams computed based on the

empirical formation enthalpies were found to strongly resemble the phase diagrams for Al-Ce, Al-Nd and Al-La assessed by Cacciamani *et al*. [6,7]. Since these results were obtained by two independent research groups on independently-assessed databases for the same systems, the disappointing agreement with experimental phase diagrams appears to be due to the (too low) empirical formation enthalpies that may have overestimated the lattice stability of the hypothetical C15 phases.

To improve the phase diagrams, two re-assessments using formation enthalpies derived from FP were undertaken. The first treatment set the enthalpy as constant and ignored the temperature dependence (i.e., parameters $b_1 = b_2 = 0$ in Eq. 4-5) of the end-members ${}^{o}G_{M:M}^{C15}$ and ${}^{o}G_{R:R}^{C15}$ with respect to the SER state. This simplification is helpful for purposes of database compatibility because their vibrational entropy cannot be reliably computed owing to the structural instability of the hypothetical lattices. We attempted to calculate the vibrational free energy for C15-Al_2Al using ATAT [41-44], but the calculation resulted in unstable modes and thus further attempts on C15-R_2R and C15-R_2M became unnecessary. In fact, the vibrational entropy of a lattice is only physically meaningful if the lattice has a stable equilibrium state, which can be defined by locating its minimum Gibb free energy at constant temperature and pressure. However, the hypothetical C15 variants are likely to be mechanically unstable and any disturbance in atomic displacement (i.e., vibration modes) would result in a continuous decrease of its Gibbs free energy. Therefore, our first treatment was to ignore their temperature dependence of Gibbs free energy. However, the temperature dependence of the ${}^{o}G_{R:M}^{C15}$ (parameters b_3 in Eq. 6) with respect to the SER state is required to order to minimize the distortion due to the sublattice remolding. Since the vibrational entropy of C15-R_2M is not

available, parameter b_3 in Eq. 6 was set to equal to the temperature coefficient of the stable ${}^{o}G_{M:R}^{C15}$ for simplicity, and was taken directly from the assessed databases [9,10,11], as suggested in Ref. [8]. The FP calculated ΔH_f values at 0 K were directly approximated as the ΔH_f at 298.15 K in this study for simplicity, as proposed by Wolverton [25,26]. The resulting distortion of the Al-Ca phase diagram becomes much smaller but the diagram is still not satisfactory (see the short-dashed lines in Fig. 1). This is due to the (relatively) very small positive value of ΔH_f = +8.7 kJ/mol for C15-Ca_2Ca (see Table 1). On the other hand, the resulting distortion of the Al-Ce and Al-Nd systems is now negligible (see the dotted lines in Fig. 2 and Fig. 3) and the agreement with the experimental phase diagrams is much improved.

In order to improve the agreement with experimental phase diagrams for cases such as the Al-Ca system, a second re-assessment was undertaken by introducing the temperature dependence of the end-members ${}^{o}G_{M:M}^{C15}$ and ${}^{o}G_{R:R}^{C15}$. They were simply set to the same value as the stable ${}^{o}G_{M:R}^{C15}$, namely $b_1 = b_2 = b_3$, as suggested in Ref. [8]. Note that the entropies of formation for C15-M_2M, R_2R and R_2M cannot be the same as for C15-M_2R because they have very different compositions, therefore, this simple treatment is not a well-founded approach and should not be used unless it is absolutely needed such as for Al-Ca system. The resulting Al-Ca phase diagram from the second treatment is represented by the dotted lines in Fig. 1. Clearly the distortion becomes very small and the second re-assessment gives acceptable agreement with experiment. For the Al-Ce and Al-Nd systems, the distortion to the phase diagram resulting from the second re-assessment is negligible and they appear as if a stoichiometric C15-A_2B_1 sublattice were used. Therefore, these lines are not shown in the figures in order to avoid confusion (although a second reassessment is unnecessary for Al-Ce and Al-Nd systems).

The same procedures described above were applied to the binary Ce-Co, Nd-Ni and Ni-Y systems to examine how phase diagrams in the TM-RE systems would change based on reevaluating the sublattice remodeling with FP formation enthalpies, shown in Figs. 5-7 respectively. When the empirical parameters were used, the remodeled C15-$(Ce,Co)_2(Ce,Co)_1$ phase exhibits a homogeneity range over 58.9-66.7 at% Co, and the temperature of the invariant peritectic reaction $Liquid + Co_3Ce \Leftrightarrow Co_2Ce$ is increased by ~11 ^{o}C. This outcome implies that the remodeled C15-$(Ce,Co)_2(Ce,Co)_1$ becomes more stable than the stoichiometric C15-$(Co)_2(Ce)_1$ when the empirical parameters were used. By contrast, when the FP results were used, the distortion to the TM-RE phase diagrams is negligible for both treatments (i.e., 1st treatment: $b_1 = b_2 = 0$; 2nd treatment: $b_1 = b_2 = b_3$ in Eq. 4-5) for all three TM-RE systems. Therefore, it seems that for TM-RE system, if the FP energetics are used, then only the temperature dependence for the hypothetical C15 antiphase needs to be considered while that for the C15 end members is not needed. This is mainly because all the hypothetical C15-R_2M lattices have a large positive ΔH_f value of 75-88 kJ/mol (see Table 1).

Finally, the enthalpies of formation for C15-M_2R and its hypothetical C15 variants from FP (see Table 1) were examined, and it was found that the energy constraint proposed in Refs. [39,40] (see Eq. 7) is not valid for systems of Al-Ca, Al-Ce, Al-Nd, Al-Y, Ce-Co and Nd-Ni, although it appears to be valid for Ni-Y at T=0 K (compare the values in 4th and 5th row in Table 1). The ΔH_f values for all C15-R_2Al lattices computed from FP are significantly smaller than those predicted on the basis of Eq. 7 (e.g. Ce_2Al), whereas the ΔH_f values for all the C15-R_2TM lattices computed from FP are larger than those predicted from Eq. 7. All the C15-R_2TM lattices

studied have a large positive ΔH_f value of 75-88 kJ/mol whereas all the C15-RE_2Al compounds have a relatively small ΔH_f value of 21-38 kJ/mol (see Table 1). The calculation results are self-consistent with the fact that the stable C15-TM_2RE has a much less negative ΔH_f than the corresponding stable C15-Al_2RE. Based on current FP calculations, it is tempting to suggest that a large positive value of ΔH_f would be required to form a hypothetical C15-AB_2 lattice if the stable C15-A_2B has a small enthalpy of formation (i.e. less negative, or weak interatomic interaction), and vice versa. This conclusion is apparently contrary to the energy constraint proposed in Refs. [39,40,5] (see Eq. 7), which implies the opposite of our conclusions based on FP calculations.

In fact, it is known that TM and RE elements tend to repel each other while Al and RE/TM tend to attract each other in Al-rich Al-TM-RE glass forming systems [45,46]. By analogy, it can be assumed that the Al-RE bonding in a C15-Al_2RE lattice is likely to be stronger than TM-RE bonding in a C15-TM_2RE lattice. The assumption can be justified by the experimental facts that C15-Al_2RE has a much more negative value of ΔH_f (at both T=0 and T=298.15 K) and that it has a very high melting point (if compared with the melting point of the pure Al and RE elements). On the other hand, the C15-TM_2RE compound has a much less negative value of ΔH_f and its melting point is lower than that of the pure TM and RE elements. Therefore, it is sensible to assume that ΔH_f for a hypothetical C15-RE_2Al should be smaller than for a hypothetical C15-RE_2TM (both are positive values).

Wagner's assumption [39] was that the molar Gibbs energy of formation of a defected ordered intermetallic phase is a linear function of the number of defects in the different sites: the

FP results suggest, however, that this assumption does not correspond to the real interatomic interactions in the ordered intermetallic phase. A set of enthalpies of formation of the hypothetical C15 end members and their antiphases that are more physically grounded can be calculated from FP, and can be used directly for CALPHAD database development. For the C15 Laves phases, including all the C15-Al_2RE, TM_2RE, Al_2Sc and Al_2Y compounds, they have been thermodynamically assessed in the literature using a stoichiometric sublattice model. However, when database compatibility is at issue in the future, the energetics from FP calculations for the hypothetical C15 lattices should be used rather than the empirical parameters in the CALPHAD community. This is particularly important when the empirical parameters fail to reproduce a reasonably accurate binary phase diagram, as in the case of the Al-Ca, Al-Ce, Al-Nd and Ce-Co systems.

5. Conclusions

FP calculations in the current study show significantly more positive energies of formation for a wide range of hypothetical C15 compounds (end members and antiphases) when compared to typical estimated values. This means that the stability of these compounds has been overestimated, which in turn means that a much exaggerated homogeneity range is predicted for the majority of the systems (especially for Al-RE systems) studied. These problems with the phase diagrams could not be corrected through re-optimization without changing the empirical parameters. On the other hand, the FP-derived enthalpies of formation for the hypothetical C15 lattices resulted in reasonable phase diagrams, such that no reoptimization is necessary for the

existing database. Further, examination of the FP energetics suggests that the Gibbs energy constraint commonly used in the CALPHAD community [3-7,39,40] is not valid for any of the systems studied except Ni-Y.

Acknowledgements

The authors would like to acknowledge financial support from the Computational Materials Science Network, a program of the Office of Science, US Department of Energy, and NDF Grant DMR-0111198. We would like to thank M. Mihalkovic, M. Zinkevich and G.J. Shiflet for useful discussions.

References

1. T.B. Massalski, H. Okamoto, P.R. Subramanian, L. Kacprzak, Binary Alloy Phase Diagrams, ASM International, Materials Park, OH 44073.
2. H. Okamoto, Desk Handbook, Phase Diagrams for Binary Alloys. ASM International, Materials Park, OH 44073.
3. M. Zinkevich, N. Mattern, I. Bacher, Z. Metallkd. 93 (2002) 186.
4. C.A. Danon, C. Servant, J. Alloys Compd. 366 (2004) 191.
5. I. Ansara, T.G. Chart, A. Fernandez Guillermet, F.H. Hayes, U.R. Kattner, D.G. Pettifor, N. Saunders, K. Zeng, CALPHAD 21 (1997) 171.
6. G. Cacciamani, R. Ferro, CALPHAD 25 (2001) 583.
7. G. Cacciamani, A.M. Cardinale, G. Borzone, R. Ferro, CALPHAD 27 (2003) 227.
8. K. Ozturk, Y. Zhong, L.Q. Chen, C. Wolverton, J.O. Sofo, Z.K. Liu, Metall. Mater. Trans. A 36 (2005) 5.
9. M.C. Gao, N. Unlu, G.J. Shiflet, M. Mihalkovic, M. Widom, Metall. Mater. Trans. A., in press, November 2005.
10. K. Ozturk, L.Q. Chen, Z.K. Liu, J. Alloys Compds. 340 (2002) 199.
11. COST 507, Thermochemical database for light metal alloys, Luxembourg: Office for Official Publications of the European Communities, 1998.
12. X.P. Su, W.J. Zhang, Z.M. Du, J. Alloys Compd. 267 (1998) 121.
13. Y. Du, N. Clavguera, CALPHAD 20 (1996) 289.
14. Z.M. Du, W.J. Zhang, J. Alloys. Compd. 245 (1996) 164.
15. B. Sundman, B. Jansson, J.O. Andersson, CALPHAD 9 (1985) 153.

16. G. Kresse, J. Hafner, Phys. Rev. B 47 (1993) 558.

17. G. Kresse, J. Furthmuller, Phys. Rev. B 54 (1996) 11169.

18. R.O. Jones, O. Gunnarsson, Rev. Mod. Phys. 61, 689 (1989).

19. M. Mihalkovic, M. Widom, Phys. Rev. B 70 (2004) 144107.

20. G. Kresse, D. Joubert, Phys. Rev. B 59 (1999) 1758.

21. J.P. Perdew, K. Burke, M. Ernzerhof, Phys. Rev. Lett. 77 (1996) 3865.

22. G. Borzone, A.M. Cardinale, G. Cacciamani, R. Ferro, Z. Metall. 84 (1993) 635.

23. WWW site http://alloy.phys.cmu.edu (see special ‘‘published’’ entries).

24. V.S. Timofeev, A.A. Turchanin, A.A. Zubkov, I.A. Tomilin, Thermochimica Acta 299 (1997) 37.

25. C. Wolverton, Acta mater. 49 (2001) 3129.

26. C. Wolverton, X.Y. Yan, R. Vijayaraghavan, V. Ozolin, Acta mater. 50 (2002) 2187.

27. Y. Zhong, C. Wolverton, Y.A. Chang, Z.K. Liu, Acta mater. 52 (2004) 2739.

28. S.H. Zhou, Y. Wang, C. Jiang, J.Z. Zhu, L.Q. Chen, Z.K. Liu, Mat. Sci. Eng. A 397 (2005) 288.

29. R. Arroyave, D. Shin, Z.K. Liu, Acta mater. 53 (2005) 1809.

30. B.L. Gyorffy, Phys. Rev. B 5 (1972) 2382.

31. F. Ducastelle, Order and Phase Stability in Alloys, Elsevier Science, New York, 1991.

32. J.M. Sanchez, F. Ducastelle, D. Gratias, Physica 128A (1984) 334.

33. D. de Fontaine, Solid State Phys. 47, 33 (1994).

34. A. Zunger, in NATO ASI on Statics and Dynamics of Alloy Phase Transformation, edited by P. E. Turchi and A. Gonis, Plenum Press, New York, 1994, Vol. 319, p. 361.

35. A. Zunger, S.H. Wei, L.G. Ferreira, J.E. Bernard, Phys. Rev. Lett. 65 (1990) 353.

36. S.H. Wei, L.G. Ferreira, J.E. Bernard, A. Zunger, Phys. Rev. B 42 (1990) 9622.

37. K.C. Hass, L.C. Davis, A. Zunger, Phys. Rev. B 42 (1990) 3757.

38. C. Jiang, C. Wolverton, J. Sofo, L.-Q.Chen, Z.-K. Liu, Phys. Rev. B 69 (2004) 214202.

39. C. Wagner, Thermodynamics of Alloys, Cambridge, Mass., USA, Addison-Wesley Press, pp. 54-66.

40. I. Ansara, N. Dupin, H.L. Lukas, B. Sundman, "Thermodynamic Modeling of the Phases in the Al-Ni System" in "Application of Thermodynamics in the Synthesis and Processing of Materials" 1994, eds. P. Nash and B. Sundman, TMS, Warrendale, PA, 1995, pp. 273-283.

41. A. van de Walle, G. Ceder, J. Phase Equil. 23 (2002) 348.

42. A. van de Walle, M. Asta, Modell. Simul. Mater. Sci. Eng. 10 (2002) 521.

43. A. van deWalle, M. Asta, G. Ceder, CALPHAD 26 (2002) 539.

44. D.B. Laks, L.G. Ferreira, S. Froyen, A. Zunger, Phys. Rev. B 46 (1992) 12587.

45. H.Y. Hsieh, B.H. Toby, T. Egami, Y. He, S.J. Poon, G.J. Shiflet, J. Mater. Res. 5 (1990) 2807.

46. A.N. Mansour, C.P. Wong, R.A. Brizzolara, Phys. Rev. B 50 (1994) 12401.

47. VASP online manual: <http://cms.mpi.univie.ac.at/vasp/vasp/vasp.html>

APPENDIX

VASP manual [47] recommends a "high" precision calculation if very small energy differences (≤10 meV) between two competing "phases", which can not be described with the same supercell, have to be calculated. It is also recommended for surface energy calculations [47]. In case of enthalpies of formation, a composition-weighted average of the pure elemental cohesive energies is subtracted from the cohesive energy of a given compound. Therefore, the overall effect of choice of precision on ΔH_f value is very small. For example, we calculated the Al-Ca system using both "high" and "medium" precision. The result on the enthalpies of formation (ΔH_f) is listed in Table 2. The change in ΔH_f is less than ±2 meV/atom for the C15-Al_2Ca, Al_2Al, $AlCa_2$, and Ca_2Ca lattices when switching precision from "high" to "medium". This change is very small, and the uncertainty of the ΔH_f value in this work is less than 10 meV/atom, therefore, "medium" precision was used in this work for efficiency in computation without lowering the overall accuracy.

Table 2: Enthalpies of formation of C15 lattices in the Al-Ca system with varying precision calculated from FP at T=0 K.

C15 Lattice	ΔH_f (meV/atom)			K-points
	High	Medium	Low	
Al_2Ca	-336.6	-338.1	-342.1	10×10×10
$AlCa_2$	+485.3	+483.5	+479.4	9×9×9
Al_2Al	+160.3	+159.3	+159.4	11×11×11
Ca_2Ca	+87.8	+88.4	+88.4	8×8×8

FIGURE CAPTIONS

Figure 1: The Al-Ca phase diagram computed using empirical parameters and FP energetics. The Ca-rich part is not shown for clear illustration. Solid lines represent the phase diagram using a stoichiometric sublattice model for the C15 phase [10]. Long-dashed lines represent the phase diagram using the empirical parameters for the hypothetical C15 phases (Eq. 8-10). Short-dashed lines represent the phase diagrams using parameters a_i taken from FP calculations and setting $b_1 = b_2 = b_3$ (Eq. 4-6). The dotted lines represent the phase diagram using parameters a_i taken from FP calculations and setting $b_1 = b_2 = 0$. The lines are consistent in Figure 1-7. In all cases, the Gibbs energy description for the stable C15-Al_2Ca is taken from Ref. [10]: $G_{Al:Ca}^{Al_2Ca} = 2/3^o G_{Al}^{fcc} + 1/3^o G_{Ca}^{fcc} - 32679 + 19.583T$.

Figure 2: The Al-Ce phase diagram. The Gibbs energy description for the stable C15-Al_2Ce is taken from Ref. [9]: $G_{Al:Ce}^{Al_2Ce} = 2/3^o G_{Al}^{fcc} + 1/3^o G_{Ce}^{fcc} - 50060 + 9.889T$.

Figure 3: The Al-Nd phase diagram. The Gibbs energy description for the stable C15-Al_2Nd is taken from Ref. [9]: $G_{Al:Nd}^{Al_2Nd} = 2/3^o G_{Al}^{fcc} + 1/3^o G_{Nd}^{dhcp} - 54037 + 11.622T$.

Figure 4: The Al-Y phase diagram. The Gibbs energy description for the stable C15-Al_2Y is taken from Ref. [11]: $G_{Al:Y}^{Al_2Y} = 2/3^o G_{Al}^{fcc} + 1/3^o G_{Y}^{hcp} - 82006 + 11.776T$. Note that there is no visible distortion to the phase equilibria when the FP-based energies were used; this holds true for Figure 5-7.

Figure 5: The Ce-Co phase diagram. The Gibbs energy description for the stable C15-Co_2Ce is taken from Ref. [12]: $G_{Co:Ce}^{Co_2Ce} = 2/3^o G_{Co}^{hcp} + 1/3^o G_{Ce}^{hcp} - 96143 + 2.972T$.

Figure 6: The Nd-Ni phase diagram. The Gibbs energy description for the stable C15-Ni_2Nd is taken from Ref. [13] for both treatments: $G_{Ni:Nd}^{Ni_2Nd} = 2/3^o G_{Ni}^{fcc} + 1/3^o G_{Nd}^{dhcp} - 35009 + 11.67T$.

Figure 7: The Ni-Y system. The Gibbs energy description for the stable C15-Ni_2Y is taken from Ref. [14] for both treatments: $G_{Ni:Y}^{Ni_2Y} = 2/3^o G_{Ni}^{fcc} + 1/3^o G_{Y}^{hcp} - 33954 + 3.055T$.

Table 1: Enthalpies of formation (ΔH_f, kJ/mol of atoms) of C15-M_2R (M=Al, Co, Ni; R=Ca, Ce, Nd, Y) compounds and their hypothetical variants calculated from FP at T=0 K.

Phase	Al-Ca	Al-Ce	Al-Nd	Al-Y	Co-Ce	Ni-Nd	Ni-Y	Comment
M_2M	15.3	15.6	15.6	15.6	19.7	21.4	21.4	FP[a]
R_2R	8.7	20.4	23.6	24.4	20.4	23.6	24.4	FP
R_2M	46.7	20.9	35.2	38.1	75.2	87.7	87.7	FP
R_2M	56.7	80.2	87.8	91.7	64.4	75.7	86.8	Eq. 7 (FP)[b]
R_2M	42.2	60.0	64.0	92.0	33.7	45.0	44.0	Eq. 10 (Empirical)[c]
M_2R	-32.7	-44.2	-48.6	-51.7	-24.3	-30.7	-41.0	FP
M_2R	-32.2	-50.0	-54.0	-82.0	-23.7	-35.0	-34.0	CALPHAD [9-14]

a: ΔH_f = +15.6 kJ/mol is recommended for C15-Al_2Al for database development purpose.

b: Data were calculated according to Eq. 7; ${}^{o}G_{M:M}^{C15}$, ${}^{o}G_{R:R}^{C15}$ and ${}^{o}G_{M:R}^{C15}$ are from FP.

c: Data were calculated according to Eq. 10, and ${}^{o}G_{M:R}^{C15}$ is from Refs. [9-14]. The empirical parameters for C15-M_2M and R_2R are set to +5 kJ/mol (see Eqs. 8 and 9).

Figure 1: Al-Ca

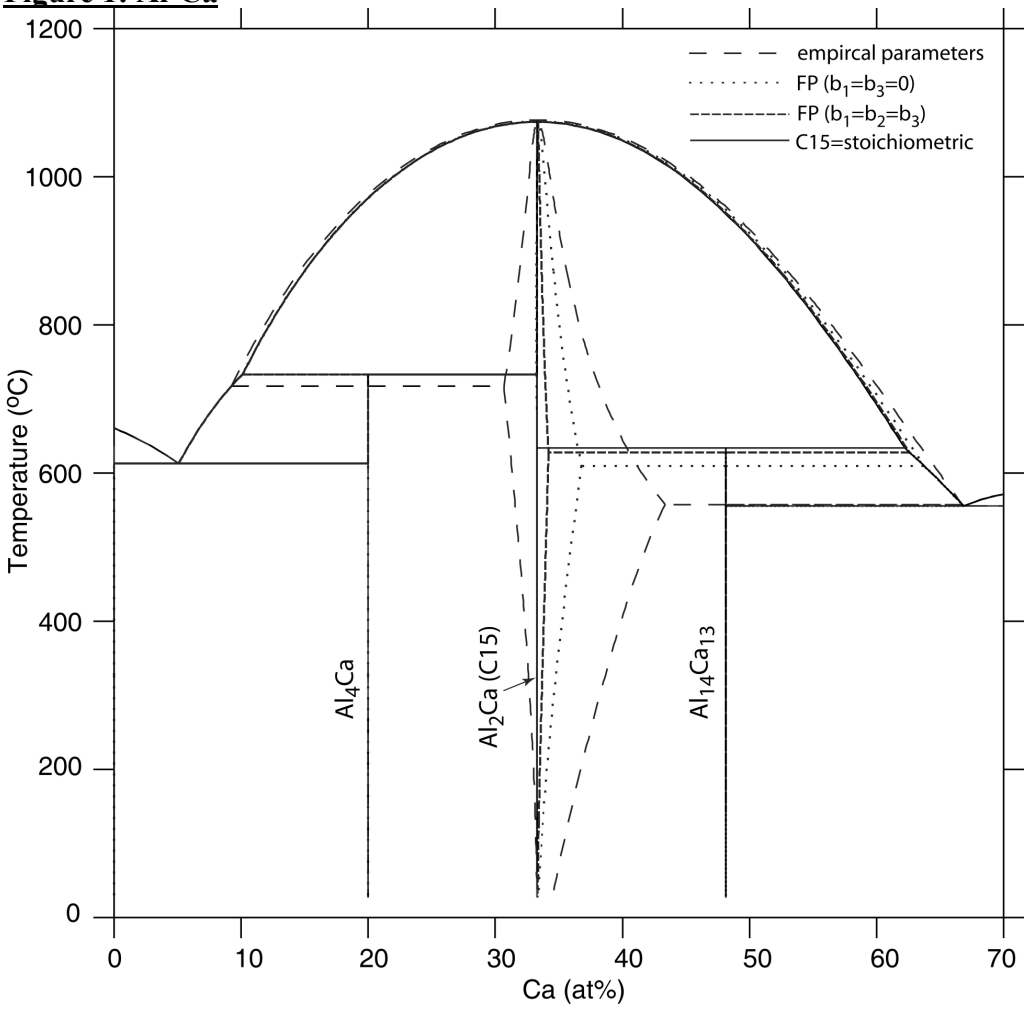

Figure 2: Al-Ce

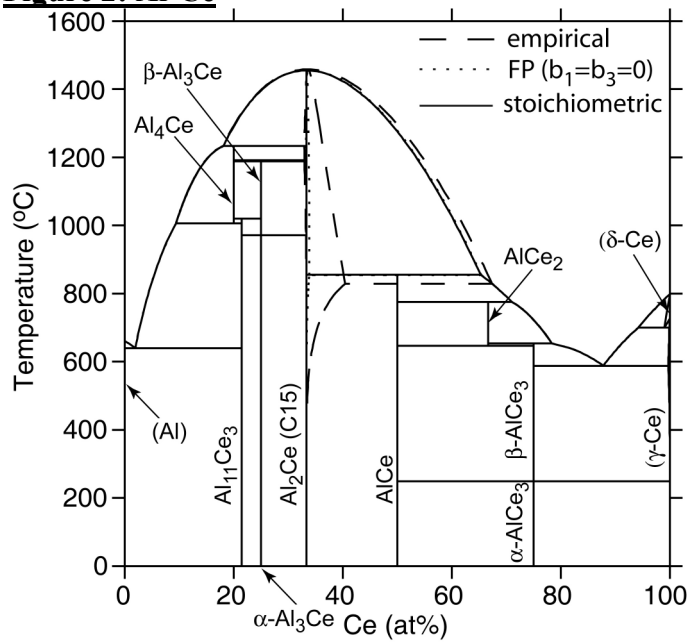

Figure 3: Al-Nd

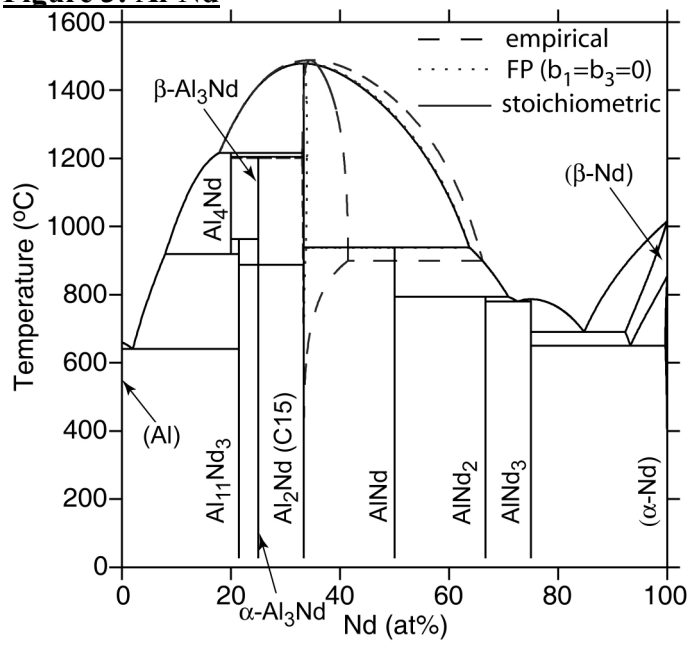

Figure 4: Al-Y

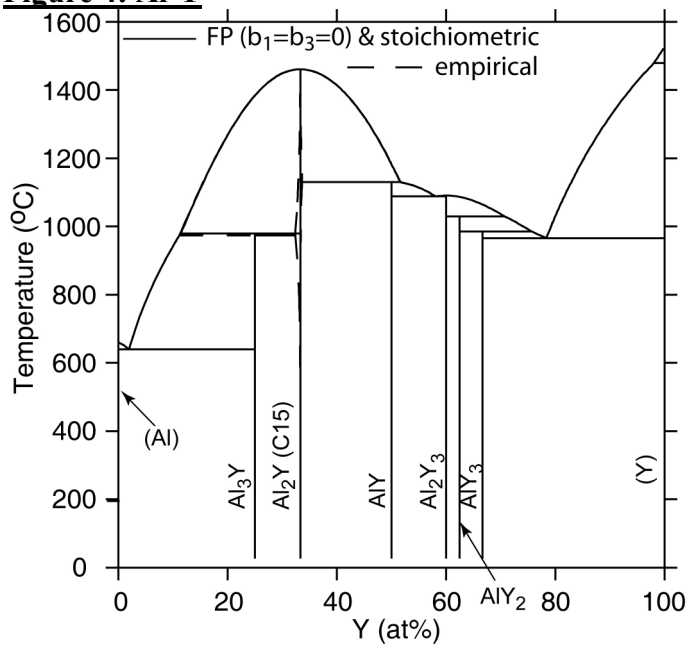

Figure 5: Ce-Co

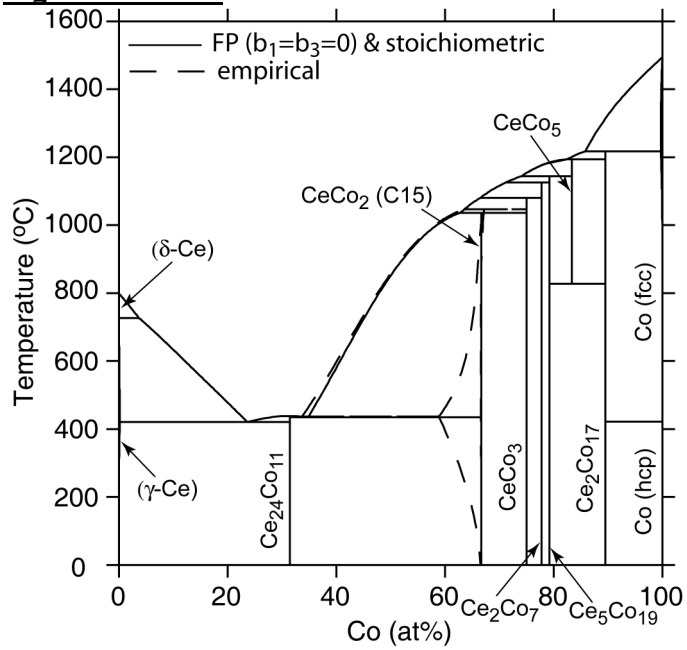

Figure 6: Nd-Ni

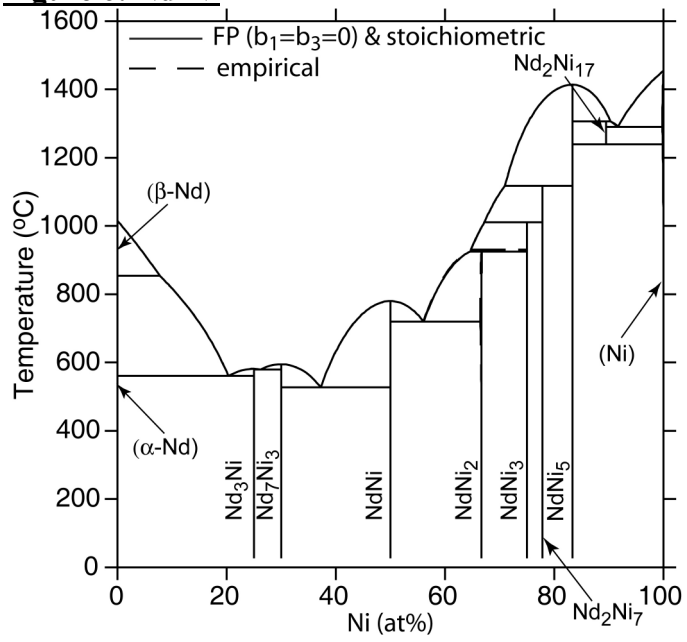

Figure 7: Ni-Y

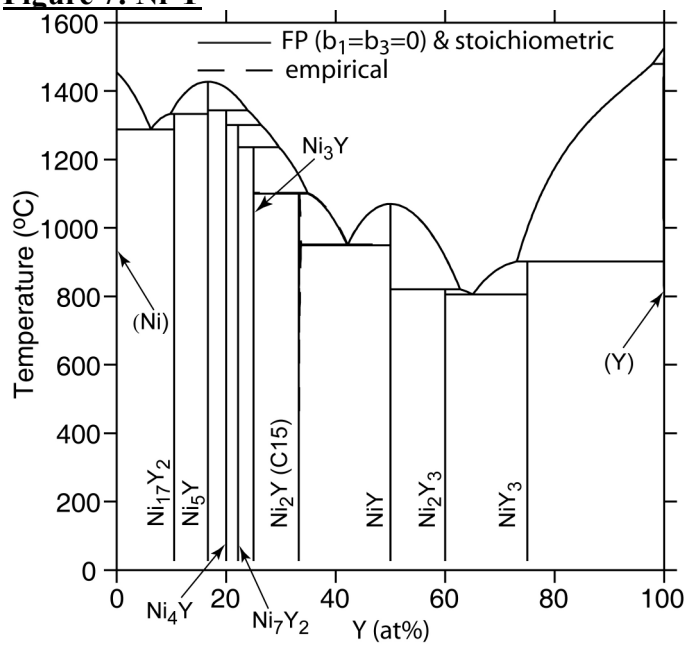
FP (b_1=b_3=0) & stoichiometric
empirical
Ni$_3$Y
(Ni)
(Y)
Ni$_{17}$Y$_2$
Ni$_5$Y
Ni$_2$Y (C15)
NiY
Ni$_2$Y$_3$
NiY$_3$
Ni$_4$Y
Ni$_7$Y$_2$
Temperature (°C)
Y (at%)
0
200
400
600
800
1000
1200
1400
1600
0
20
40
60
80
100